Ser. **429**, 444 (1990).
7. J. M. Hayes, K. H. Freeman, B. N. Popp, C. H. Hoham, *Org. Geochem.* **10**, 1115 (1990).
8. K. H. Freeman, J. M. Hayes, J. M. Trendel, P. Albrecht, *Nature* **343**, 254 (1990).
9. The sample set consists of three subsamples of the bituminous marl (marls 1 to 3), a sample from the stromatolitic limestone, and a sample from the massive gypsum from the same evaporitic cycle (Fig. 4). The geology of this basin is extensively described by G. B. Vai and F. R. Ricci Lucci [*Sedimentology* **24**, 211 (1977)].
10. The freeze-dried samples were powdered and Soxhlet extracted with methanol:CH_2Cl_2 (1:7.5 by volume for 40 hours) under nitrogen. Saturated hydrocarbon, alkylthiophene, alkylsulphide, and polar fractions were isolated from the extracts as in (*11*) and analyzed using GC and GC-MS after addition of internal standards prior to fractionation (*6*).
11. M. E. L. Kohnen, J. S. Sinninghe Damsté, A. C. Kock-van Dalen, J. W. de Leeuw, *Geochim. Cosmochim. Acta* **55**, 1375 (1991).
12. Portions of the polar, alkylthiophene, and alkylsulphide fractions were desulfurized with Raney Ni and subsequently hydrogenated as described previously (*14*). To release ether-bound carbon skeletons a portion (~35 mg) of the polar fraction of marl-2 was dissolved in a 57% HI aqueous solution and refluxed for 2 hours. The alkyliodides obtained were isolated [R. V. Panganamala, C. F. Sievert, D. G. Cornwell, *Chem. Phys. Lipids* **7**, 336 (1971)] and reduced with $LiAlH_4$ [modified after J. E. Johnson, R. H. Blizzard, H. W. Carhart, *J. Am. Chem. Soc.* **70**, 3664 (1948)].
13. The isotope-ratio-monitoring GC-MS system is described in (*7, 8*). A fused silica capillary column (50 m by 0.32 mm) coated with cross-linked methyl silicone gum (Ultra-1, film thickness 0.52 μm) was used with He as carrier gas to analyze the fractions of marl-2 (Fig. 4). In the case of the alkylthiophene and the alkylsulphide fraction both the untreated and desulfurized fractions were analyzed.
14. J. S. Sinninghe Damsté, W. I. C. Rijpstra, J. W. de Leeuw, P. A. Schenck, *Org. Geochem.* **13**, 593 (1988).
15. The S-containing heterocycles isolated from the Vena del Gesso sediments have five-, six-, and seven-membered rings containing four or five adjacent C atoms and one to three S atoms. These include thiophenes (C_4S ring, aromatic) and the saturated thiolanes (C_4S), thianes (C_5S), dithianes (C_4S_2), and trithiepanes (C_4S_3).
16. S. Liaaen-Jensen, in *Marine Natural Products*, D. J. Faulkner and W. H. Fenical, Eds. (Academic Press, New York, 1978), pp. 1–73; S. Liaaen-Jensen, in *Photosynthetic Bacteria*, R. K. Clayton and W. R. Sistrom, Eds. (Plenum, New York, 1978), pp. 233–247.
17. S. G. Wakeham, *Geochim. Cosmochim. Acta* **54**, 1325 (1990).
18. $\delta^{13}C = 10^3[(R_x - R_s)/R_s]$, where $R = {}^{13}C/{}^{12}C$, x designates sample, s designates PDB standard and $R_s = 0.0112372$.
19. E. E. Bray and E. D. Evans, *Geochim. Cosmochim. Acta* **22**, 2 (1961).
20. G. Eglinton, R. J. Hamilton in *Chemical Plant Taxonomy*, T. Swain, Ed. (Academic Press, New York, 1963), pp. 187–208.
21. B. N. Popp, R. Takigiku, J. M. Hayes, J. W. Louda, E. W. Baker, *Am. J. Sci.* **289**, 436 (1989).
22. J. J. Boon *et al.*, *Nature* **277**, 125 (1979).
23. P. Deines, in *Handbook of Environmental Isotope*, P. Fritz and J. C. Fontes, Eds. (Elsevier, Amsterdam, 1980), vol. 1A, pp. 329–406.
24. J. K. Volkman, G. Eglinton, E. D. S. Corner, T. E. Forsberg, *Phytochemistry* **19**, 2619 (1980).
25. P. Metzger, C. Berkaloff, E. Casavall, A. Coute, *ibid.* **24**, 2305 (1985).
26. W. G. Deuser, *Nature* **225**, 1069 (1970).
27. S. J. Rowland, D. A. Yon, C. A. Lewis, J. R. Maxwell, *Org. Geochem.* **8**, 207 (1985).
28. J. S. Sinninghe Damsté, E. R. van Koert, A. C. Kock-van Dalen, J. W. de Leeuw, P. A. Schenck, *Org. Geochem.* **14**, 555 (1989); M. E. L. Kohnen *et al.*, *Geochim. Cosmochim. Acta* **54**, 3053 (1990).
29. P. D. Nichols, J. K. Volkman, A. C. Palmisano, G. A. Smith, D. C. White, *J. Phycol.* **24**, 90 (1988).
30. L. Quandt, G. Gottschalk, H. Ziegler, W. Stichler, *FEMS Microbiol. Lett.* **1**, 125 (1977); R. Sirevag, B. B. Buchanan, J. A. Berry, J. H. Troughton, *Arch. Microbiol.* **112**, 35 (1977); R. E. Summons and T. G. Powell, *Geochim. Cosmochim. Acta* **51**, 557 (1987); *Nature* **319**, 763 (1986).
31. P. Metzger and E. Casadevalle, *Tetrahedron Lett.* **28**, 3931 (1987).
32. G. Holzer, J. Oro, T. G. Tornabene, *J. Chromatogr.* **186**, 795 (1979); T. G. Tornabene, T. A. Langworthy, G. Holzer, J. Oro, *J. Mol. Evol.* **13** (1979); J. B. Risatti, S. J. Rowland, D. A. Yon, J. R. Maxwell, *Org. Geochem.* **6**, 93 (1984).
33. S. C. Brassell, A. M. K. Wardroper, I. D. Thomson, J. R. Maxwell, G. Eglinton, *Nature* **290**, 693 (1981).
34. E. S. Deevey and M. S. Stuiver, *Limnol. Oceanogr.* **9**, 1 (1964); T. Torgerson, D. E. Hammond, W. B. Clarke, T.-H. Peng, *ibid.* **26**, 110 (1981).
35. G. Ourisson, P. Albrecht, M. Rohmer, *Pure Appl. Chem.* **51**, 709 (1979); G. Ourisson, P. Albrecht, M. Rohmer, *Trends Biochem. Sci.* **7**, 236 (1982).
36. M. De Rosa and A. Gambacorta, *Prog. Lipid Res.* **27**, 153 (1988).
37. M. De Rosa *et al.*, *Biochim. Biophys. Acta* **875**, 487 (1986).
38. R. S. Oremland, L. M. Marsh, S. Polcin, *Nature* **296**, 143 (1982).
39. Supported in part by the Netherlands Foundation for Earth Science Research (AWON) with financial aid from the Netherlands Organization for Scientific Research (NWO). We thank M. Baas, A. H. Knol-Kalkman, W. Pool, M. P. Ricci, and S. A. Studley for technical and analytical assistance. M.E.L.K. acknowledges the EAOG for a travel scholarship. Delft Organic Geochemistry Unit Contribution 251.

24 October 1991; accepted 3 February 1992

Contact Electrification and Adhesion Between Dissimilar Materials

Roger G. Horn and Douglas T. Smith

Simultaneous measurements of surface force and surface charge demonstrate strong attraction due to the spontaneous transfer of electrical charge from one smooth insulator (mica) to another (silica) as a result of simple, nonsliding contact in dry nitrogen. The measured surface charge densities are 5 to 20 millicoulombs per square meter after contact. The work required to separate the charged surfaces is typically 6 to 9 joules per square meter, comparable to the fracture energies of ionic-covalent materials. Observation of partial gas discharges when the surfaces are approximately 1 micrometer apart gives valuable insight into the charge separation processes underlying static electrical phenomena in general.

Contact electrification, manifest as static or triboelectricity, is a well-known effect whose consequences can be very irksome or very beneficial depending on the circumstances. Despite the familiarity and importance of this phenomenon, there is limited understanding of the fundamental mechanisms by which charge transfers from one insulator to another during contact and remains there as the materials are separated (*1, 2*).

Particles and surfaces are charged intentionally in such applications as photocopying, laser printing, electrostatic precipitation, and particle separation processes, which make use of electrostatic forces to promote adhesion. However, the notion that spontaneous charge transfer between materials in contact acts to increase adhesion between them has received little attention despite the efforts of Derjaguin *et al.* (*3*) and the work of Dickinson and coworkers (*4*) demonstrating that charge separation occurs during interfacial fracture.

We report an experimental method based on the use of a surface force apparatus (*5*) with in situ electrometers (*6*), which enables both surface forces and surface charges to be measured. Two smooth dissimilar insulating materials are brought into contact and separated; direct measurements are made of the charge transferred during contact and of the resulting electrostatic attractive force. These experiments demonstrate and quantify the attraction that results from contact electrification and show that the work required to separate two charged surfaces in a dry atmosphere is comparable to the work required to fracture the individual materials. This work of adhesion depends on how much excess charge remains on the surfaces after a series of discharges across the gap between the materials as they are separated through the micrometer range.

Two thin (1 to 10 μm), transparent solids are mounted as crossed cylinders of radius ≈20 mm in the surface force apparatus. For these experiments we used one sheet of atomically smooth mica and one of fused silica (*7*), prepared by a blown-bubble method that gives near-atomic smoothness (*8*). Solid-solid separation D is controlled and measured with subnanometer accuracy by interferometry (*9*) between silver coat-

Ceramics Division, National Institute of Standards and Technology, Gaithersburg, MD 20899.

ings on the back surfaces (Fig. 1A). The two solids in contact flatten elastically over a certain area, measurable from interference fringes (*10*); because the surfaces are smooth, this is taken to be the true contact area. To determine the sign and quantity of charge residing on the front surfaces of the solids, electrical contacts are made with the silver coatings. As the solids are separated, the surface charge induces image charge in the silver (Fig. 1B). The image charge, readily measured by electrometers, increases in magnitude from zero when the solids are touching to the full surface charge when they are far apart (6).

Surface charge densities from 5 to 20 mC/m^2 (or 1 electronic charge per 8 to 32 nm^2) were measured for simple, nonsliding contacts between silica and mica in dry nitrogen gas (*11*). These values are unusually high compared to most contact electrification measurements (*1*) because of the smooth, clean, and thin solids used here (6). The measured charges on the two materials were always equal in magnitude, silica becoming negative and mica positive. The charging process could be repeated many times, implying that the supply of charge carriers is replenishable and hence most likely to be electrons.

The effect of spontaneous charge transfer on the force between silica and mica in dry nitrogen is illustrated in Fig. 2. No charge was detected by the electrometers when the two materials first approached, and the only force was van der Waals attraction. However, after the surfaces made contact, a large pull-off force of −67 mN was required for their initial separation, and a strong attractive force persisted over several micrometers. For comparison, the pull-off force between two mica surfaces of comparable radii of curvature is −12 mN (*10*), and −9 mN for two silica surfaces (*12*); the range of attraction in either case does not exceed 0.1 μm. The strong, long-range mica-silica attraction is always associated with the presence of opposite charges on the two materials as detected by the electrometers: the force is evidently electrostatic. No comparable charge transfer is observed with mica-mica and silica-silica contacts.

The electrostatic attraction is strong enough to deform the materials elastically, bending the thin solids and stretching the epoxy glue that holds them to cylindrical glass lenses. This slight "pointing" effect, amounting to ≈25 nm per surface at small separations, is readily detected by the optical interferometer (*12*). With two similar materials, no deformation is observed.

Close examination of the separation force (Fig. 2) reveals certain values of D at which the magnitude of the attraction decreased abruptly. Concomitant reductions in surface charge of 10 to 20% (~10 pC) were observed at each of these separations; otherwise, the charge remained constant (*13*). The abrupt reductions in charge were equal and opposite on the two front surfaces, indicative of partial discharges across the gap between the solids, rather than through either solid substrate. These discharges (discussed below) occurred only when D reached certain values. The discharge separations were somewhat variable from experiment to experiment, but the first was always in the range 0.5 to 0.8 μm. Time does not appear to be an important factor: no discharges occurred while the surfaces were held at fixed separations up to 3 μm for periods from 5 to 800 s. Furthermore, discharges never occurred while separation was being reduced.

An approximate analysis of the distance dependence of electrostatic force in this experimental geometry is possible if certain simplifying assumptions are made. First, surface deformation is ignored. Second, the two surfaces are modeled as infinite parallel plates, because the gap size (0 to 5 μm) is much smaller than both the diameter of the charged area (~100 μm) and the cylinders' radii of curvature (~20 mm). Third, the charge density of the plates is assumed to be uniform and equal to the total charge divided by the maximum contact area.

In calculating the force, one must consider four layers of charge: the two front surfaces plus two grounded silver electrodes a few micrometers behind them. As the solids are moved apart, image charge accumulates in each electrode and the electric field across each solid increases. The field across the gap decreases even with constant charge on the front surfaces, in contrast to the constant field between parallel plates in a normal two-layer capacitor bearing fixed charges. The force per unit area F_A at surface separation D is given by

$$F_A = -\frac{\sigma_s^2}{2\epsilon_0}\left(\frac{B}{B+D}\right)^2 \qquad (1)$$

where σ_s is the magnitude of charge per unit area on each front surface, ϵ_0 is the permit-

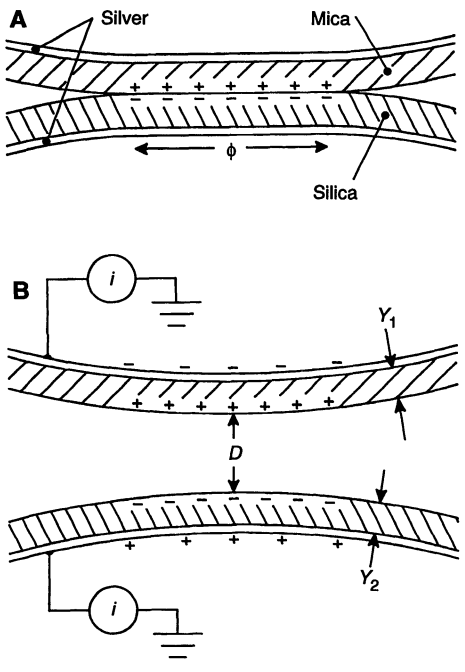

Fig. 1. (**A**) Schematic arrangement of thin solid films in the surface force apparatus. Surface separation D, solid thicknesses Y_1 and Y_2 (each ~1 to 10 μm), and contact diameter ϕ (typically 100 μm) are measured from optical interference between silver layers on the outer surfaces; silver layers are also used as electrodes. (**B**) Upon separation, charges on the front surfaces induce image charges in each silver layer. Integrating the current i flowing to each grounded electrode as the solids are separated to $D >> Y_1, Y_2$ determines the surface charge (*6*).

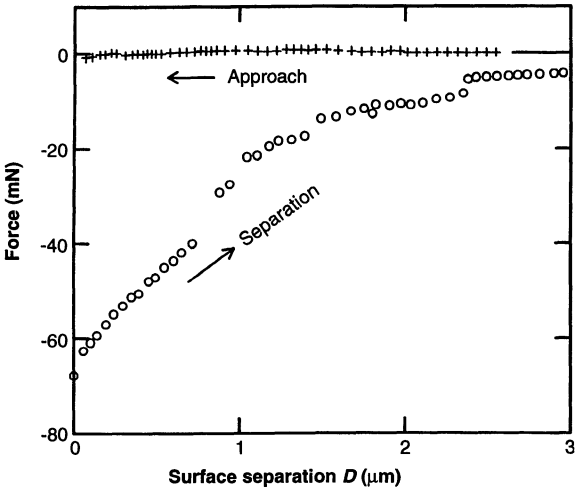

Fig. 2. Force measured between crossed cylinders of mica (radius 21.3 mm) and silica (radius 16.4 mm) in dry nitrogen gas, as a function of separation between closest points on opposite surfaces. Negative force corresponds to attraction. When the materials are brought together for the first time, there is little force between them (+). However, strong attractive forces (○) are measured on separating the surfaces from contact; these forces are ascribed to electrostatic attraction after charge transfer between the materials. Note the breaks in the data at certain separations (0.75, 0.97, 1.44, and 2.36 μm). Both charge and force build up over several (five to ten) successive contacts even though the same area of surface is brought into contact each time; the data shown here are measured after ten touches.

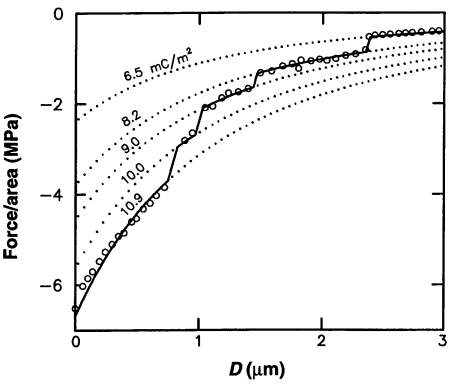

Fig. 3. The separation data from Fig. 2 replotted as force per unit area (using the measured contact area of 1.04×10^{-8} m^2), together with a series of theoretical curves (Eq. 1). Each curve corresponds to a constant surface charge density σ_s, and the values (indicated on the figure) are consistent with electrometer measurements. The mica and silica have thicknesses of 3.23 and 6.37 μm and dielectric constants of 6.6 and 3.82, respectively, giving $B = 2.16$ μm. At certain separations there are partial discharges across the gas gap, and the force jumps from one curve to another at lower charge density. Lines connecting different curve segments have the slope of the measuring spring stiffness (1.0×10^5 N/m) divided by contact area. Integrating the force defined by the solid curve segments from $D = 0$ to 3 μm gives a work of adhesion of 6.6 J/m^2.

tivity of free space, and $B \equiv Y_1/K_1 + Y_2/K_2$, with Y_1, Y_2 and K_1, K_2 the thicknesses and relative dielectric constants of the two substrates, respectively.

Figure 3 replots the separation data from Fig. 2 normalized by contact area, together with five curves representing Eq. 1 for different σ_s. The data are fitted by a sequence of constant-charge curve segments, with abrupt steps from each charge density to the next lower value at the discharge separations. Charge densities required to fit the data are within the range measured by the electrometer (*14*), and the reductions at each step are 10 to 20%, consistent with the partial discharges noted above.

A striking result of these experiments is the large work of adhesion, W, obtained by integrating the electrostatic force as a function of separation (*15, 16*). The area defined by the solid line in Fig. 3 corresponds to $W = 6.6$ to 8.8 J/m^2, the lower value obtained by assuming that the surfaces discharge completely just outside the present range of measurements (3 μm) and the higher value by assuming that no further discharges occur beyond 3 μm. This value for W is comparable to the work of cohesion of ionic and ionic-covalent solids obtained from fracture experiments (*17*). For example, fracture energies in dry nitrogen are 8.7 J/m^2 for silica (*18*) and 1 to 2 J/m^2 for mica (*19, 20*). In contrast, surface force apparatus measurements of adhesion between two like surfaces (determined primarily by van der Waals or capillary forces rather than the original solid bonding) are equal to only 0.08 J/m^2 for silica (*12*) and 0.11 J/m^2 for mica (*10*).

This experiment demonstrates that contact electrification can lead to strong adhesion. In general, electrostatic adhesion and other static electrical phenomena will require (i) charge transfer in contact and (ii) subsequent charge separation. The amount of charge transferred in contact depends on many factors, including material type, electronic structure, defects, adsorbates, surface roughness, and sliding. The amount of charge separated is limited by two possible recombination processes: tunneling as the surfaces are first separated and discharges across larger gaps. Tunneling, if it occurs, is not detected by the present electrometer arrangement, which measures surface charges at larger separations. However, it may be no coincidence that the measured charge densities create electric fields across the gap (0.6×10^9 to 2.3×10^9 V/m) that are comparable to typical field emission strengths: fields may be limited to these values by tunneling across subnanometer gaps (*16*) as the surfaces are first separated.

Discharges occurring between separating charged surfaces have been observed before (*4, 21*), but not at such small distances as those reported here. What is interesting and important is that no discharges occur until the gap reaches micrometer dimensions, despite the fact that the electric field is very strong in much smaller gaps. The explanation can be found in theories of electric breakdown of gases (*22*). Breakdown at small gaps (the left side of the Paschen curve) occurs when a small number of initiatory electrons are amplified by an avalanche mechanism involving ionizing collisions with gas molecules. Until the gap is comparable to the mean free path of electrons in the gas, there will be no discharge even at high field strength. In support of this, we have observed that, when the mean free path is reduced (by increasing the nitrogen pressure), the first discharge separation decreases. At atmospheric pressure the surface charge survives to micrometer gaps (*23*), and, because the discharges are only partial, the materials retain some charge when they are separated to larger distances.

REFERENCES AND NOTES

1. J. Lowell and A. C. Rose-Innes, *Adv. Phys.* **29**, 947 (1980).
2. J. E. Stern, B. D. Terris, H. J. Mamin, D. Rugar, *Appl. Phys. Lett.* **53**, 2717 (1988).
3. B. V. Derjaguin, N. A. Krotova, V. P. Smilga, *Adhesion of Solids* (Consultants Bureau, New York, 1978).
4. K. A. Zimmerman, S. C. Langford, J. T. Dickinson, *J. Appl. Phys.* **70**, 4808 (1991).
5. J. N. Israelachvili and G. E. Adams, *J. Chem. Soc. Faraday Trans. 1* **74**, 975 (1978).
6. D. T. Smith, *J. Electrostat.* **26**, 291 (1991).
7. Suprasil F100, Heraeus-Amersil, Buford, GA. Use of this product does not imply its endorsement by the National Institute of Standards and Technology.
8. R. G. Horn, D. T. Smith, W. Haller, *Chem. Phys. Lett.* **162**, 404 (1989).
9. R. G. Horn and D. T. Smith, *Appl. Opt.* **30**, 59 (1991).
10. R. G. Horn, J. N. Israelachvili, F. Pribac, *J. Colloid Interface Sci.* **115**, 480 (1987).
11. An open vessel of P_2O_5 was kept in the body of the apparatus, and a continuous flow of dry, filtered N_2 gas was maintained throughout the experiments.
12. D. T. Smith and R. G. Horn, *Mater. Res. Soc. Symp. Proc.* **170**, 3 (1990).
13. At least on the time scale of the measurements. The decay rate of surface charge in dry N_2 is many hours (*6*).
14. Closer comparison between the fitted and measured charges is impracticable because our electrometer technique does not monitor the absolute charge at every separation during force measurements.
15. The work of adhesion defined here is not equal to the Dupré reversible work of adhesion given by $W_D = \gamma_{1E} + \gamma_{2E} - \gamma_{12}$, where the γ values are interfacial energies between the three combinations of solids 1 and 2 and the environment E. The surfaces of silica and mica after separation are not at thermodynamic equilibrium, because they still carry surface charge.
16. Charged surfaces represent the equilibrium configuration only at small separations; the crossover between uncharged and charged surfaces resembles the harpooning phenomenon described in theories of atomic collisions [J. W. Gadzuk, *Comments At. Mol. Phys.* **16**, 219 (1985)].
17. B. R. Lawn, *Fracture of Brittle Solids* (Cambridge Univ. Press, London, ed. 2, 1992), table 3.1.
18. S. M. Wiederhorn, *J. Am. Ceram. Soc.* **52**, 99 (1969).
19. K.-T. Wan, N. Aimard, S. Lathabai, R. G. Horn, B. R. Lawn, *J. Mater. Res.* **5**, 172 (1990).
20. Mica cleavage does not occur in our experiments, because that process involves a stronger bonding force (acting over a shorter distance) than the maximum force sustained by the silica-mica interface.
21. R. Elsdon and F. R. G. Mitchell, *J. Phys. D* **9**, 1445 (1976); X. Ji, Y. Takahashi, Y. Komai, S. Sheet, *J. Electrostat.* **23**, 381 (1989).
22. F. Llewellyn-Jones, *Ionization and Breakdown in Gases* (Methuen, London, 1957). Extension of the theory to small gaps is discussed by A. B. Parker and P. C. Johnson [*Proc. R. Soc. London Ser. A* **325**, 511 (1971)] and D. Bhasavanich and A. B. Parker [*ibid.* **358**, 385 (1977)].
23. The first discharge in Fig. 3 occurs at $D_s = 0.75$ μm with a potential across the gap calculated as 690 V, so the field is $E = 9.2 \times 10^8$ V/m. The gas number density is $n = 2.7 \times 10^{25}$ m^{-3}, giving $nD_s = 2.0 \times 10^{-19}$ m^{-2} and $E/n = 3.4 \times 10^{-17}$ V/m^2. B. M. Jelenković and A. V. Phelps [*Phys. Rev. A* **36**, 5310 (1987)] indicated an average distance between ionizing collisions for electrons in N_2 of at least 10 μm at comparable E/n. These investigators measured discharge at 690 V in N_2 between stainless steel and sintered carbon electrodes at nD_s values corresponding to gaps five times those reported here. This discrepancy is not understood; it may be related to differences in electrode materials.

24. We acknowledge valuable discussions with D. Y. C. Chan, B. N. Cox, J. T. Dickinson, J. W. Gadzuk, J. N. Israelachvili, B. R. Lawn, G. M. McClelland, A. S. de Reggi, and R. J. van Brunt; experimental assistance from A. Grabbe; and the generous gift of silica samples from Heraeus-Amersil. Supported under Office of Naval Research contract N0014-88-F-0034.

6 January 1992; accepted 3 March 1992